

1 Article

# 2 Multi-Rate Real-Time Simulation Method Based on 3 the Norton Equivalent

4 Junjie Zhu\*, Bingda Zhang

5 The Key Laboratory of Smart Grid of Ministry of Education, Tianjin University, Tianjin 300072, China;

6 jjzhu@tju.edu.cn (J.Z.); bdzhang@tju.edu.cn (B.Z.);

7 \* Correspondence: jjzhu@tju.edu.cn; Tel.: +86-182-2206-9101

8 **Abstract:** For the problem of poor accuracy of the existing multi-rate simulation methods, this paper  
9 proposes a multi rate real-time simulation method based on the Norton equivalent, compared with  
10 multi-rate simulation method based on the ideal source equivalent. After the Norton equivalence of  
11 the fast subsystem and the slow subsystem, they are obtained simultaneously at the junction nodes.  
12 In order to reduce the amount of simulation calculation, the Norton equivalent circuit is obtained  
13 by incremental calculation. The data interface between the fast subsystem and the slow subsystem  
14 is realized by extrapolation method. For ensuring the real-time performance of the simulation, the  
15 method that the slow subsystem calculates ahead of the fast subsystem is given for the slow  
16 subsystem with a large amount of calculation. Finally, the AC/DC hybrid power system was  
17 simulated on the real-time simulation platform (FRTDS), and the simulation results were compared  
18 with the single-rate simulation, which verified the correctness and accuracy of the method.

19 **Keywords:** multi-rate real-time simulation; the ideal source equivalent; the Norton equivalent;  
20 increment; extrapolation method  
21

---

## 22 1. Introduction

23 China has built the world's largest AC/DC hybrid power system with the highest voltage level,  
24 and the regional power grids have been interconnected through Ultra-high voltage AC / DC  
25 transmission lines [1,2]. The control and protection system plays an important role in the safe and  
26 reliable operation of AC/DC hybrid power system, and the real-time simulation technology based on  
27 hardware in the loop can be used to verify the correctness of the protection device action and the  
28 effectiveness of the control strategy [3,4].

29 Large-scale AC/DC hybrid power system contain a large number of power electronic devices.  
30 Compared with traditional AC power system, these devices have a small time scale, and their  
31 dynamic characteristics have a great impact on the safe and stable operation of the power system. In  
32 order to simulate power electronic equipment more accurately, the simulation step size is required  
33 to be smaller and smaller [5]. This is a challenge for the simulation of AC/DC hybrid power system.  
34 For improving the speed of simulation, two aspects are generally considered, one is to reduce the  
35 amount of simulation calculation, the other is to use parallel computing technology. Ref [6] proposed  
36 a multi-layer topology hybrid model for power electronic switching components, which allows a  
37 large number of single switches to be reduced to only two diodes and controlled voltage and current  
38 sources. This greatly reduces the number of switching combinations and the size of the generated  
39 code, and improves the speed of simulation. Ref [7] proposed a method of GPU based parallel matrix  
40 exponential algorithm for large scale power system electromagnetic transient simulation, which  
41 significantly improves the simulation calculation speed. However, the GPU cannot independently  
42 complete the process control and data scheduling in the simulation calculation process, so it needs to  
43 cooperate with the CPU to complete the simulation calculation [8]. The above methods are all single-  
44 rate electromagnetic transient simulation methods, ignoring the differences in the time scale of power  
45 equipment in different systems. The selection of simulation step size can only be based on the system

46 with the smallest time scale of power equipment, which will cause serious waste of computing  
47 resources. [9].

48 In view of the above problems, scholars at home and abroad have proposed the concept of  
49 parallel multi-rate electromagnetic transient computing, and different simulation steps are adopted  
50 for different systems according to the time scale of power equipment in the system [10–12]. Ref [13]  
51 proposed a multi-rate electromagnetic transient simulation method based on Latency technology, in  
52 which the external part of the subnet was modeled as an ideal source. As the ideal source model  
53 could not guarantee that the node signals (voltage and current) on both sides of the interface were  
54 equal, the simulation accuracy was reduced. Ref [14] proposed a node splitting interface (NSI) multi-  
55 rate parallel technology. It solves the state space equations of fast and slow subnets simultaneously,  
56 avoiding data prediction and signal delay, and improving the simulation accuracy, but the method  
57 cannot be used for real-time simulation. The above multi-rate simulations are all offline simulations  
58 and cannot be used for hardware-in-the-loop experiments. Ref [15] proposed a multi-rate real-time  
59 simulation method based on a joint simulation platform of real-time digital simulator (RTDS) and  
60 field programmable gate array (FPGA). It uses the asynchronous interaction method that FPGA data  
61 transmission is appropriately earlier than RTDS data transmission, which reduces a certain  
62 communication delay. But the communication delay problem of data interaction between different  
63 platforms still exists, which causes the reduction of simulation accuracy. In Ref [16] a FPGA based  
64 MR real-time simulation of MMC-HVDC grids is proposed. The MMC system is decoupled by a stub-  
65 line, and each MMC valve is implemented on one FPGA. The FPGAs can select different time steps  
66 to meet the requirement of the time constraints. However, using multiple FPGA blocks for simulation  
67 calculation will not only cause data synchronization problem and decrease the simulation accuracy,  
68 but also waste the hardware resources of FPGA.

69 For the problem of poor accuracy of the existing multi-rate simulation methods, this paper  
70 proposes a multi rate real-time simulation method with the Norton equivalent circuit based on multi-  
71 rate simulation method with the ideal source equivalent. After the Norton equivalence of the fast  
72 subsystem and the slow subsystem, they are obtained simultaneously at the junction nodes. In order  
73 to reduce the amount of simulation calculation, the Norton equivalent circuit is obtained by  
74 incremental calculation. The data interface between the fast subsystem and the slow subsystem is  
75 realized by extrapolation method. Finally, the AC/DC hybrid power system was simulated on the  
76 real-time simulation platform (FRTDS), which verified the correctness and accuracy of the method.

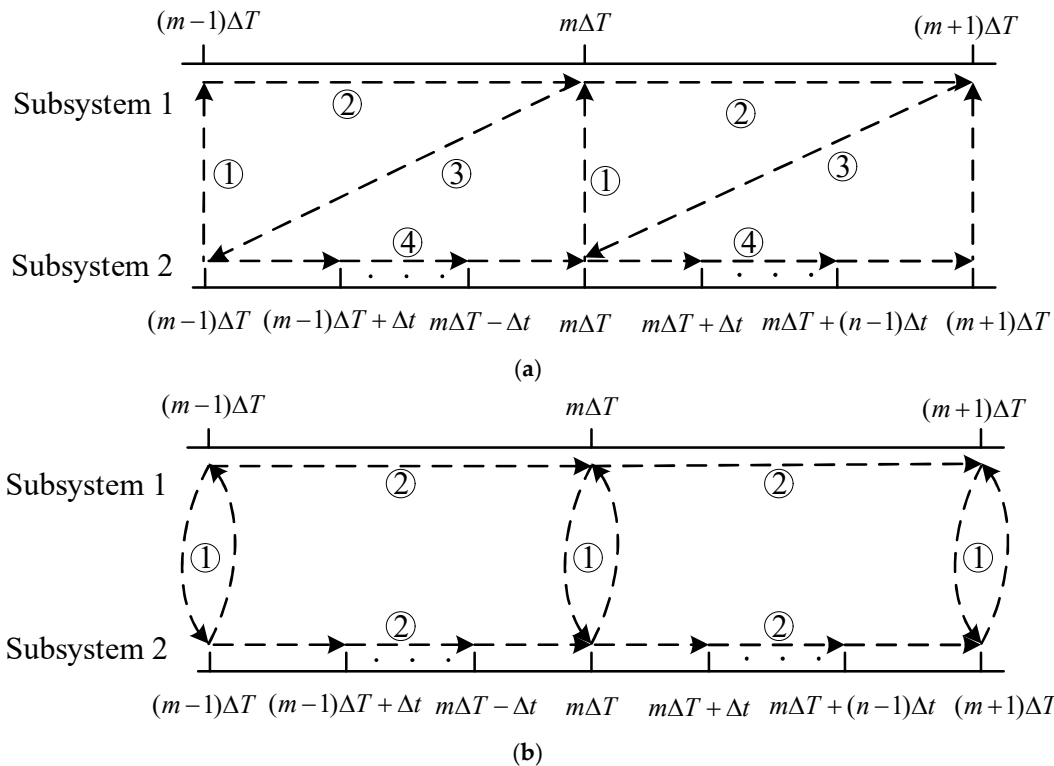
## 77 2. Multi-rate Simulation Calculation Timing

78 In the AC/DC hybrid power system, the power electronic equipment with fast control  
79 characteristics and the AC large-scale power grid are intertwined in different time scale processes,  
80 which makes the operation and control characteristics of the AC/DC hybrid power system more  
81 complicated [17]. Therefore, in the simulation of the AC/DC hybrid power system, various time scale  
82 processes in the AC/DC hybrid power grid should be considered. The simulation must be able to  
83 simulate the fast electromagnetic transient process (time scale of a few microseconds) of power  
84 electronic equipment such as converters and static synchronous compensators. It is also necessary to  
85 be able to simulate the switching process of the converter valve of the DC power system and the  
86 electromagnetic transient process of the AC power system (time scale of tens of microseconds to  
87 hundreds of microseconds) [18,19]. When using a single simulation step to simulate an AC/DC hybrid  
88 power system. If the simulation step is too small, the amount of calculation that needs to be completed  
89 within a single step is too large to complete. If the simulation step size is too large, the dynamic  
90 characteristics of the power electronic components cannot be simulated, which reduces the accuracy  
91 of the simulation. For balancing the accuracy of simulation and the scale of simulation, the entire  
92 system is decomposed into multiple subsystems. According to the time scale of the power equipment  
93 in the subsystem, different step sizes are used for simulation calculation, that is, multi-rate  
94 simulation.

95 There are two types of multi-rate simulation calculation timing: serial calculation timing and  
96 parallel calculation timing. Figure 1 shows the serial calculation timing and parallel calculation

97 timing of the two subsystems. Among them, Subsystem 1 uses a larger simulation step size  $\Delta T$ , and  
 98 Subsystem 2 uses a smaller simulation step size  $\Delta t$ , where  $\Delta T = n\Delta t$  ( $n$  is a positive integer).

99  
 100



101  
 102

103 **Figure 1.** Simulation calculation timing. (a) Serial calculation timing. (b) Parallel computing timing

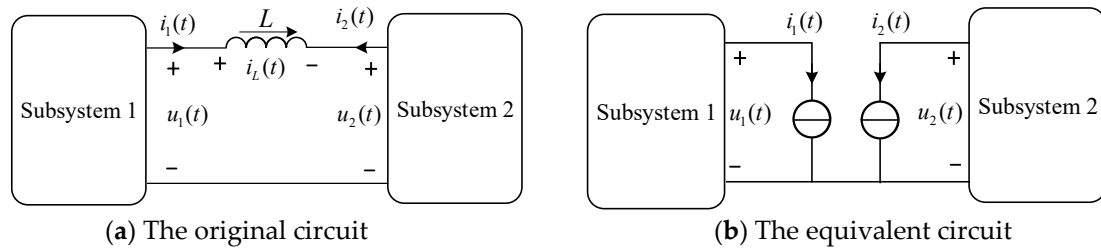
104 In multi-rate simulation, the calculation tasks of serial calculation timing need to be completed  
 105 in sequence. In Figure 1(a), ① at the time of  $(m-1)\Delta T$ , subsystem 2 transmits the data to subsystem 1  
 106 through the interface; ② Subsystem 1 uses the received data for simulation calculation; ③  
 107 Subsystem 1 transfers the data to Subsystem 2 through the interface; ④ Subsystem 2 uses the  
 108 received data for simulation calculation. In serial calculation, the calculation tasks ①, ②, ③ and ④  
 109 need to be completed in sequence, which seriously affects the speed of simulation calculation.  
 110 Therefore, the serial calculation sequence can generally only be used for offline simulation, not for  
 111 real-time simulation calculation.

112 The task of parallel computing time sequence can be completed at the same time, which  
 113 improves the computing speed. In Figure 1(b), ① at the time of  $(m-1)\Delta T$ , subsystem 1 and  
 114 Subsystem 2 conduct data interaction; ② Subsystem 1 uses the received data for one simulation  
 115 calculation, while subsystem 2 uses the received data for  $n$  times of simulation calculation. In  
 116 Subsystem 2, the data required by the simulation calculation is not known and more prediction data  
 117 is required, so the parallel multi-rate simulation accuracy is low. However, for ensuring the real-time  
 118 nature of multi-rate simulation, only parallel calculation timing can be used.

### 119 3. Multi-rate real-time simulation based on the Norton equivalence

#### 120 3.1. Multi-rate Real-time simulation method based on the ideal source equivalence

121 In the multi-rate real-time simulation of the power system, the inductance and capacitor element  
 122 can be equivalent to the ideal source and the system is decoupled into multiple independent  
 123 subsystems by taking advantage of the fact that the inductance current and capacitance voltage in the  
 124 circuit cannot be suddenly changed. For example, the circuit with inductance  $L$  is equivalent as  
 125 shown in Fig. 2.



126  
127

128 **Figure 2.** The equivalent diagram of capacitor branch.  $i_L(t)$  is the current with inductance  $L$ .  $u_1(t)$ ,  $u_2(t)$  is the  
129 voltage across the inductance  $L$ . At this time, the inductance  $L$  is equivalent to an ideal current source, and the  
130 system is decoupled into two independent subsystems, as shown in Figure 2(b).

131 The relationship between current  $i_L(t)$  and voltage  $u_1(t)$ ,  $u_2(t)$  with inductance  $L$  is as follows in  
132 Fig. 2(a).

$$133 \quad u_1(t) - u_2(t) = L \frac{di_L}{dt} \quad (1)$$

134 Assuming that Subsystem 1 uses a larger simulation step size  $\Delta T$ , and Subsystem 2 uses a  
135 smaller simulation step size  $\Delta t$ , where  $\Delta T = n\Delta t$  ( $n$  is a positive integer). By using Euler method to  
136 differentiate equation 1, then we can find:

$$137 \quad i_L(t) = i_L(t - \Delta T) + \frac{\Delta T}{L} \times [u_1(t) - \frac{1}{n} \sum_{k=1}^n u_2(t - \Delta T + k\Delta t)] \quad (2)$$

138 At the time of  $m\Delta T$ , Subsystem 1 and Subsystem 2 exchange and synchronize information. The  
139 voltage  $u_1(t)$  and  $u_1(t - \Delta T)$  of Subsystem 1 is sent to Subsystem 2, and the voltage  $u_2(t - \Delta T + k\Delta t)$   
140 ( $k=1,2,\dots,n$ ) of Subsystem 2 is sent to Subsystem 1. Then perform data synchronization according to  
141 the substitution theorem, namely  $i_1(t) = -i_2(t) = i_L(t)$ . After that, the calculation can be divided into two  
142 parallel tasks. The voltage and current of the equivalent current source of Subsystem 1 and Subsystem  
143 2 are obtained simultaneously.

144 For Subsystem 1, the current  $i_1(t + \Delta T)$  of the equivalent current source can be represented as:

$$145 \quad i_1(t + \Delta T) = i_1(t) + \frac{\Delta T}{L} [u_1(t) - u_2(t)] \quad (3)$$

146 According to the current  $i_1(t + \Delta T)$  of Subsystem 1, calculate the voltage  $u_1(t + \Delta T)$  of Subsystem 1.

147 For subsystem 2, the current  $i_2(t + k\Delta t)$  of the equivalent current source can be represented as:

$$148 \quad i_2(t + k\Delta t) = i_2(t + (k-1)\Delta t) + \frac{\Delta t}{L} [-u_1(t + (k-1)\Delta t) + u_2(t + (k-1)\Delta t)] \quad (4)$$

149 Where  $u_2(t + (k-1)\Delta t)$  and  $i_2(t + (k-1)\Delta t)$  are the voltage and current of the equivalent current source  
150 in Subsystem 2 and they are known. However, the current  $u_1(t + (k-1)\Delta t)$  in Subsystem 1 is unknown,  
151 and it can be estimated by extrapolation. Then the extrapolation formula is:

$$152 \quad u_1(t + (k-1)\Delta t) = u_1(t) + \frac{k-1}{n} [u_1(t) - u_1(t - \Delta T)] \quad (5)$$

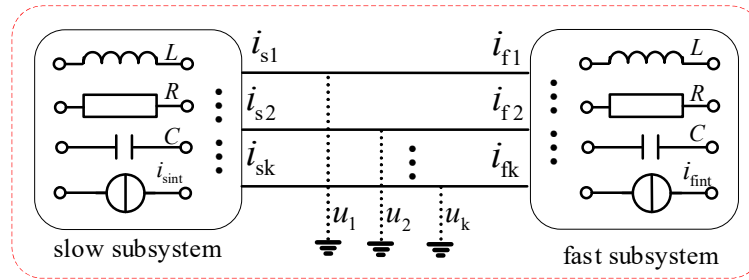
153 According to the current  $i_2(t + k\Delta t)$  of Subsystem 2, calculate the voltage  $u_2(t + k\Delta t)$  of Subsystem 2.

154 After that, the simulation of the next moment will be continued. Similarly, the calculation  
155 process of multi-rate simulation method with capacitor  $C$  can be obtained. The multi-rate simulation  
156 method with the ideal source equivalence takes advantage of the fact that the state variables of the  
157 inductors and capacitors in the system can not be changed suddenly, and they are equivalent to the  
158 ideal source model. Then, the whole system is decoupled by substitution theorem. However, in the  
159 simulation calculation, the voltage and current of the ideal source are all predicted, so the accuracy  
160 of this method is very low.

### 161 3.2. Multi-rate Real-time simulation method based on the Norton equivalence

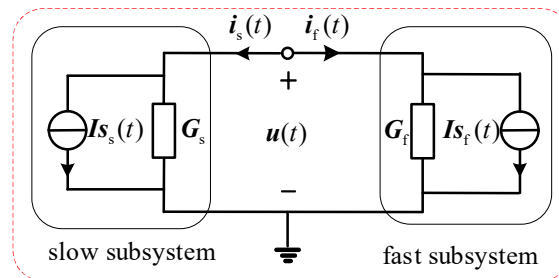
162 For the problem of the accuracy with the ideal source equivalent method, the idea of the Norton  
163 equivalent is used to replace the ideal source equivalent. After the Norton equivalence of the fast  
164 subsystem and the slow subsystem, they are obtained simultaneously at the junction nodes, and then  
165 the state variables in the sub system are obtained.

166 There are two linear sources-containing subsystems. A subsystem has a small time scale,  
 167 represented by the subscript f. The other subsystem has a larger time scale, denoted by subscript s.  
 168 The two subsystems are connected to each other through k nodes, as shown in Figure 3.



169 **Figure 3.** The diagram of power system. The input of the slow subsystem and the fast subsystem consists of two  
 170 parts, the independent current source inside the subsystem, and the voltage or current at the interface. Where  $\mathbf{i}_s$   
 171 and  $\mathbf{i}_f$  are the current vectors at the subsystem interface;  $\mathbf{u}$  is the voltage vector at the subsystem interface;  $\mathbf{i}_{sint}$   
 172 and  $\mathbf{i}_{fint}$  are the independent current source vectors inside the subsystem.

174 The Norton equivalent is applied to the slow subsystem and the fast subsystem, and the  
 175 simulation diagram based on the Norton equivalent is as shown in Figure 4.



176 **Figure 4.** Simulation diagram based on the Norton equivalent circuit

178 Assuming that the slow subsystem uses a larger simulation step size  $\Delta T$ , and the fast subsystem  
 179 uses a smaller simulation step size  $\Delta t$ , where  $\Delta T = n\Delta t$  ( $n$  is a positive integer). The Norton equivalent  
 180 circuit of the slow subsystem and the fast subsystem can be expressed as:

$$181 \quad \mathbf{i}_s(t) = \mathbf{G}_s \mathbf{u}(t) + \mathbf{I}_{s_s}(t) \quad (6)$$

$$182 \quad \mathbf{i}_f(t) = \mathbf{G}_f \mathbf{u}(t) + \mathbf{I}_{s_f}(t) \quad (7)$$

183 Where,  $\mathbf{i}_s(t)$  and  $\mathbf{i}_f(t)$  are the current vectors at the Norton equivalent circuit interface;  $\mathbf{u}(t)$  are the  
 184 voltage vector at the Norton equivalent circuit interface;  $\mathbf{G}_s$  and  $\mathbf{G}_f$  are the admittance matrix of the  
 185 Norton equivalent circuit, which are related to the state of dynamic elements in the slow subsystem  
 186 and the fast subsystem.  $\mathbf{I}_{s_s}(t)$  and  $\mathbf{I}_{s_f}(t)$  are the current sources of the Norton equivalent circuit, and  
 187 they are linear combinations of individual current sources and historical current sources.

188 So the current sources of the Norton equivalent circuit  $\mathbf{I}_{s_s}(t)$  and  $\mathbf{I}_{s_f}(t)$  can be represented as:

$$189 \quad \mathbf{I}_{s_s}(t) = \mathbf{C}_s \mathbf{x}_s(t - \Delta T) + \mathbf{D}_s \mathbf{i}_{sint}(t) \quad (8)$$

$$190 \quad \mathbf{I}_{s_f}(t) = \mathbf{C}_f \mathbf{x}_f(t - \Delta t) + \mathbf{D}_f \mathbf{i}_{fint}(t) \quad (9)$$

191 Where,  $\mathbf{x}_s(t - \Delta T)$  and  $\mathbf{x}_f(t - \Delta t)$  are the state variables at the previous moment in the slow subsystem  
 192 and the fast subsystem.  $\mathbf{i}_{sint}(t)$  and  $\mathbf{i}_{fint}(t)$  are the independent current sources at the moment in the  
 193 slow subsystem and the fast subsystem.  $\mathbf{C}_s$ ,  $\mathbf{D}_s$ ,  $\mathbf{C}_f$  and  $\mathbf{D}_f$  are the parameter matrix.

194 On the interface between the slow subsystem and the fast subsystem, there is:

$$195 \quad \mathbf{i}_s(t) = -\mathbf{i}_f(t) \quad (10)$$

196 From formula (6), (7) and (10), we can find:

$$197 \quad (\mathbf{G}_s + \mathbf{G}_f) \mathbf{u}(t) = -[\mathbf{I}_{s_s}(t) + \mathbf{I}_{s_f}(t)] \quad (11)$$

198 Where equation (11) is called the voltage equation of the interface node. From equation (11), the  
 199 voltage vector of the interface between the slow subsystem and the fast subsystem is obtained. After  
 200 that, the state variables  $\mathbf{x}_s$  and  $\mathbf{x}_f$  in the slow subsystem and the fast subsystem can be calculated.

201 When  $t = m\Delta T$  ( $m$  is a positive integer), the state of each dynamic element in the two subsystems  
 202 and the state variables  $\mathbf{x}_s(m\Delta T - \Delta T)$  and  $\mathbf{x}_f(m\Delta T - \Delta T)$  at the previous moment of the two subsystem  
 203 are known. Then the Norton equivalent is applied to the two subsystems, and calculate  $\mathbf{G}_s$ ,  $\mathbf{I}_s(t)$ ,  $\mathbf{G}_f$   
 204 and  $\mathbf{I}_f(t)$ . The voltage of the interface node can be obtained by the equation (11). Finally, the state  
 205 variables of the whole network is obtained.

206 When  $t = m\Delta T + k\Delta T$  ( $k=1,2,\dots,n-1$ ), the state of each dynamic element in the two subsystems and  
 207 the state variables  $\mathbf{x}_f(m\Delta T + (k-1)\Delta T)$  at the previous moment of the fast subsystem are known.  
 208 However, the state variables  $\mathbf{x}_s(m\Delta T - \Delta T + k\Delta T)$  of the slow subsystem are unknown. We can  
 209 calculate it as followed by extrapolation.

$$210 \quad \mathbf{x}_s(m\Delta T - \Delta T + k\Delta T) = \mathbf{x}_s(m\Delta T) + \frac{k}{n}[\mathbf{x}_s(m\Delta T) - \mathbf{x}_s(m\Delta T - \Delta T)] \quad (12)$$

211 For the slow subsystem, the parameter matrix  $\mathbf{G}_s$  corresponds to the state of the dynamic  
 212 element at time of  $(m-1)\Delta T + k\Delta T$  to  $m\Delta T + k\Delta T$ , which spans two periods. For simplifying the  
 213 calculation, the dynamic element state at time  $m\Delta T$  is used to solve the Norton equivalent of the  
 214 slow subsystem, namely  $\mathbf{G}_s(m\Delta T + k\Delta T) = \mathbf{G}_s(m\Delta T)$ . When solving the current sources of the Norton  
 215 equivalent circuit, for reducing the amount of calculation, the current sources  $\mathbf{I}_s(m\Delta T + k\Delta T)$  is  
 216 obtained by interpolation through  $\mathbf{i}_{\text{shint}}(m\Delta T)$  and  $\mathbf{i}_{\text{shint}}(m\Delta T + \Delta T)$ , instead of  $\mathbf{i}_{\text{shint}}(m\Delta T + k\Delta T)$ . the  
 217 current sources  $\mathbf{I}_s(m\Delta T + k\Delta T)$  can be expressed as:

$$218 \quad \mathbf{I}_s(m\Delta T + k\Delta T) = \mathbf{I}_s(m\Delta T) + k\Delta \mathbf{I}_s(m\Delta T) \quad (13)$$

219 Where the increment of equivalent current source  $\Delta \mathbf{I}_s(m\Delta T)$  can be represented as:

$$220 \quad \Delta \mathbf{I}_s(m\Delta T) = \frac{1}{n} \{ \mathbf{C}_s[\mathbf{x}_s(m\Delta T - \Delta T) - \mathbf{x}_s(m\Delta T - 2\Delta T)] + \mathbf{D}_s[\mathbf{i}_{\text{shint}}(m\Delta T + \Delta T) - \mathbf{i}_{\text{shint}}(m\Delta T)] \} \quad (14)$$

221 It is obvious that the current source of the Norton equivalent circuit only need be calculated once in  
 222 a large simulation step size, and the remaining current source can be obtained by the increment of  
 223 equivalent current source. Therefore, does not need to use parameter matrix frequently calculate  
 224 them, which greatly reduces the amount of calculation.

225 It can be seen from the previous analysis that the solution of the voltage equation with the  
 226 interface node requires the Norton equivalent of the fast subsystem and the slow subsystem.  
 227 Therefore, the conductance and current source with the Norton equivalent of the slow subsystem  
 228 need to be sent to the fast subsystem to solve the node voltage of the interface. After the node voltage  
 229 of the interface is solved, it needs to be sent to the slow subsystem to solve the internal state variables.  
 230 When  $t=m\Delta T$ , summarizing the above solution process, the process of the multi-rate real-time  
 231 simulation method based on the Norton equivalent is as follows:

232 (1) Calculate the Norton equivalent circuit of the slow subsystem and the fast subsystem at the  
 233  $k$ th ( $k=0,1,2,\dots,n-1$ ), period.

$$234 \quad \begin{cases} \mathbf{I}_s(t+k\Delta T) = \mathbf{C}_s \mathbf{x}_s(t-\Delta T) + \mathbf{D}_s \mathbf{i}_{\text{shint}}(t) & k=0 \\ \mathbf{I}_s(t+k\Delta T) = \mathbf{I}_s(t) + k\Delta \mathbf{I}_s(t) & k \neq 0 \end{cases} \quad (15)$$

$$235 \quad \mathbf{I}_f(t+k\Delta T) = \mathbf{C}_f \mathbf{x}_f(t+(k-1)\Delta T) + \mathbf{D}_f \mathbf{i}_{\text{fint}}(t+k\Delta T) \quad (16)$$

236 (2) According to  $\mathbf{G}_s$ ,  $\mathbf{G}_f$ ,  $\mathbf{I}_s(t+k\Delta T)$  and  $\mathbf{I}_f(t+k\Delta T)$ , write the voltage equation of the interface  
 237 node.

$$238 \quad (\mathbf{G}_s + \mathbf{G}_f) \mathbf{u}(t+k\Delta T) = -[\mathbf{I}_s(t+k\Delta T) + \mathbf{I}_f(t+k\Delta T)] \quad (17)$$

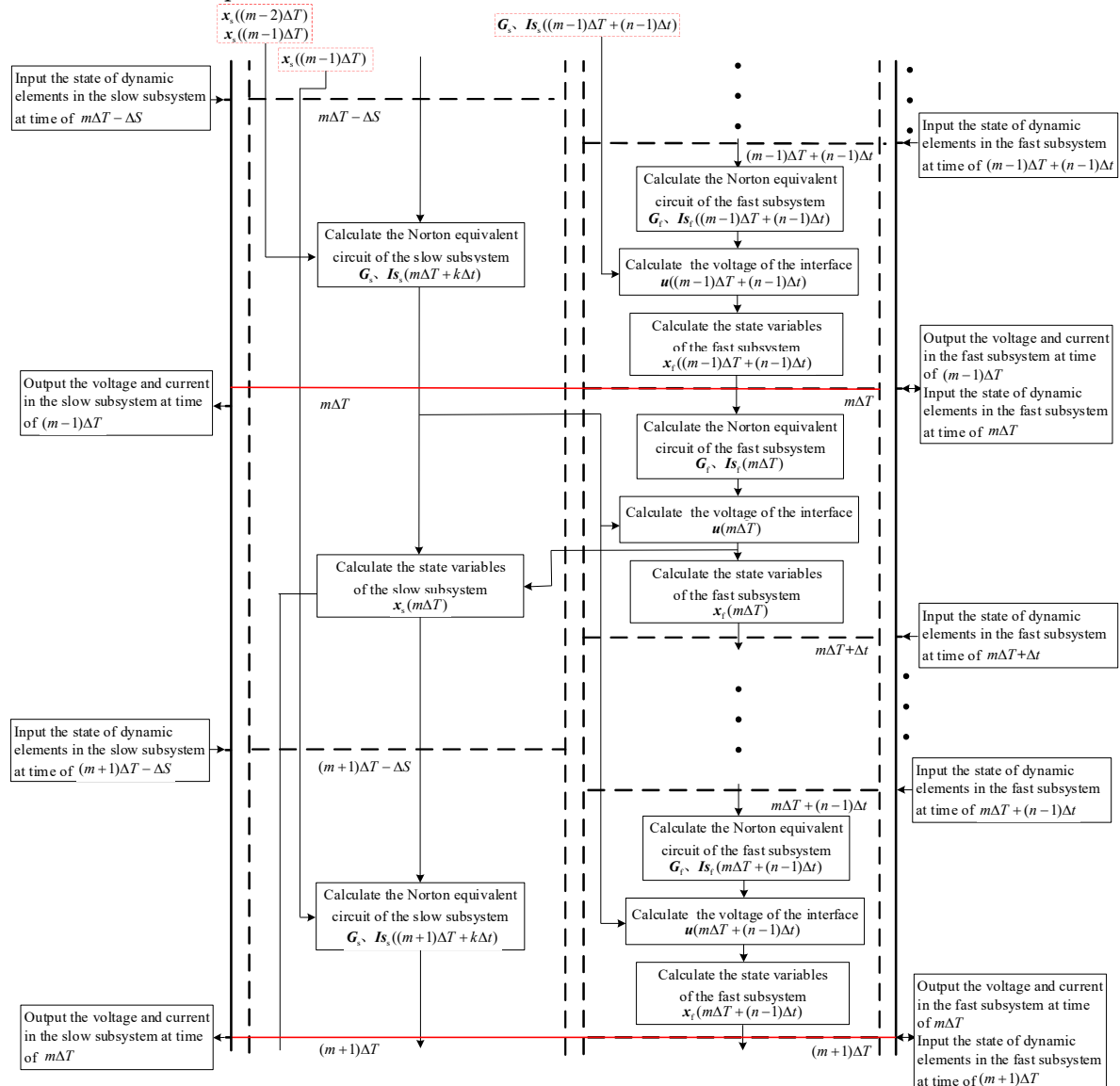
239 (3) Solve the voltage equation of the interface node to get the voltage of the interface node  
 240  $\mathbf{u}(t+k\Delta T)$ .

241 (4) According to  $\mathbf{u}(t+k\Delta T)$ , the state variable  $\mathbf{x}_f(t+k\Delta T)$  of the fast subsystem can be obtained,  
 242 and the state variable  $\mathbf{x}_s(t)$  of the slow subsystem also can be obtained.

### 243 3.3. The data interaction of multi-rate simulation.

244 For hardware-in-the-loop simulation, all calculations of a step size must be completed within  
 245 the specified time. Otherwise, the real-time performance of the simulation cannot be perfect. In the

246 multi-rate real-time simulation method based on the Norton equivalent, the Norton equivalent circuit  
 247 parameters of the slow subsystem and the fast subsystem are used to solve the voltage of interface  
 248 node. However, compared with the fast subsystem, there are many nodes the slow subsystem. The  
 249 calculation amount of solving the Norton equivalent circuit is very large, and it is difficult to complete  
 250 in a small step size. Since the slow subsystem is an AC power system, it is not very important for the  
 251 moment of state change of dynamic elements. In order not to delay the solution of the interface node  
 252 voltage, the calculation of the slow subsystem can be earlier than the fast subsystem. For the time  $\Delta S$   
 253 of the earlier solving the slow subsystem, it can be assumed that  $\Delta S = 0.5\Delta T$ . If the calculation of the  
 254 slow subsystem cannot be completed, we should gradually increase  $\Delta S$ . Otherwise, gradually  
 255 decrease until the optimal  $\Delta S$  is found.



256  
 257 **Figure 5.** the time of input and output and the logical relationship of calculation tasks with multi-rate real-time  
 258 simulation method based on the Norton equivalent.

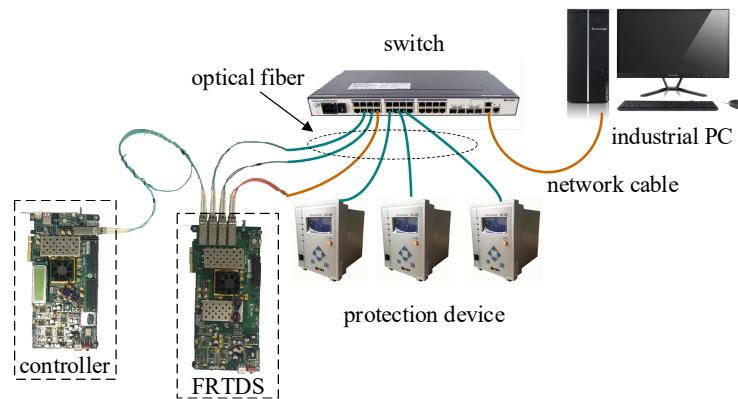
259 It can be seen from Figure 5 that within a smaller simulation step size, the Norton equivalent  
 260 circuit of the fast subsystem, the voltage of the interface node, and the state variables of the fast  
 261 subsystem must be completed. The Norton equivalent circuit of the slow subsystem, the voltage of  
 262 the interface node, and the state variables of the slow subsystem must be completed within a larger  
 263 simulation step size. In each smaller simulation step size (except the node of the larger simulation  
 264 step size), it is necessary to predict the Norton equivalent circuit parameters of the slow subsystem  
 265 for the solution of the voltage of the interface node.

### 266 3. Case Study

#### 267 3.1 Real-time simulation platform FRTDS

268 FRTDS (FPGA based Real-Time Digital Solver) is an electromagnetic transient real-time  
 269 simulation device developed by the Key Laboratory of the Ministry of Education for Smart Grid of  
 270 Tianjin University. It encapsulates commonly calculation formulas and functions in the  
 271 microprocessor core, and convert simulation scripts into instructions that control the operation of the  
 272 microprocessor core by self-developed compilation software. In order to improve the efficiency of  
 273 writing simulation scripts, a graphical modeling tool for real-time simulation of power systems has  
 274 been developed. The power system database can be generated by using the graphical modeling tool,  
 275 and then the FTRDS simulation script can be further generated, which further reduces the workload  
 276 of the researchers. Users only need to generate power system database with graphical modeling tools,  
 277 and do not need the capabilities of FPGA programming.

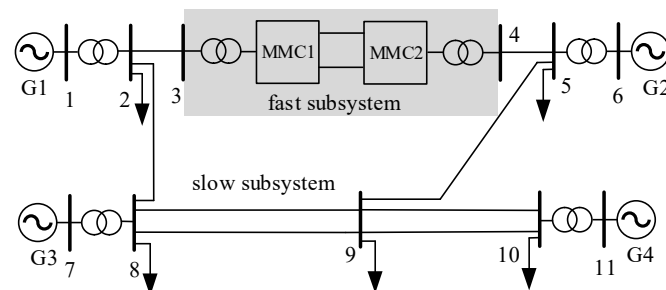
278 The UDP communication protocol is used between FRTDS and the simulated industrial  
 279 computer, the IEC61850 communication protocol is used between FRTDS and the real digital  
 280 protection device, and the Aurora communication protocol of Xilinx is used between FRTDS and the  
 281 independently developed experimental controller. The FRTDS real-time simulation platform selects  
 282 Xilinx's Virtex-7 FPGA VC709 as the solver development board. The working frequency is 200MHz.  
 283 The compilation system, the script generation system and the operation monitoring system in the  
 284 industrial PC are all developed by the QT C++ platform. The hardware-in-the-loop experimental  
 285 platform based on FRTDS is shown in Figure 6.



286  
 287 **Figure 6.** Structure of hardware in the loop simulation system based on FRTDS

### 288 3.2 Simulation System and Result

289 The four-machine AC/DC hybrid system shown in Figure 7 is selected as the simulation example.  
 290 The larger simulation step size of  $50 \mu\text{s}$  is selected for AC system, including generator, transformer,  
 291 line and load, *etc.* The smaller simulation step size of  $10 \mu\text{s}$  is selected for DC system, including  
 292 converter transformer, MMC converter station, DC line, DC filter, reactive power compensation  
 293 capacitor, *etc.*



294  
 295 **Figure 7.** Four-machine AC/DC hybrid system

296 In the AC/DC hybrid system, the converter is MMC with 77 level. The MMC is modulated by  
 297 the nearest level modulation (NLM). The MMC1 is controlled by the constant active power and the  
 298 constant reactive power. The MMC2 is controlled by the constant DC voltage and the constant  
 299 reactive power. The relevant parameters of AC/DC hybrid system are shown in Table 1.

300

name	parameter
------	-----------

The rated capacity of converter /MVA	500
The rated voltage of AC grid /kV	230
The rated capacity of converter transformer /MVA	700
The frequency of AC grid /Hz	50
The inductance of bridge legs /mH	50
The number of MMC sub-modules	76
The capacitance of MMC sub-modules /mF	3
The rated voltage of DC grid /kV	±320
The capacitance of DC line /μF	1

301 **Table 1.** The relevant parameters of AC/DC hybrid system

302 For verifying the correctness and effectiveness of the multi-rate real-time simulation method,  
 303 single-rate simulation method with the simulation step size of  $10\ \mu\text{s}$  (method 1) and two multi-rate  
 304 simulation methods are carried out for AC/DC hybrid system. Multi-rate real-time simulation  
 305 method based on the ideal source equivalence is method 2 and multi-rate real-time simulation  
 306 method based on the Norton equivalence is method 3. For single-rate simulation, FRTDS provides  
 307 2000 maximum instruction clocks. For multi-rate simulation, the memory space is opened with the  
 308 simulation step size of the slow subsystem. FRTDS provides 10000 maximum instruction clocks. The  
 309 software provided by FRTDS is used to write simulation scripts of single-rate and multi-rate methods  
 310 respectively, and then the tasks are assigned. The list of instruction space occupied by the calculation  
 311 task is shown in Table 2.

	The number of maximum instruction clocks	The number of task instruction clocks
method 1	2000	2810
method 2	10000	9080
method 3	10000	9530

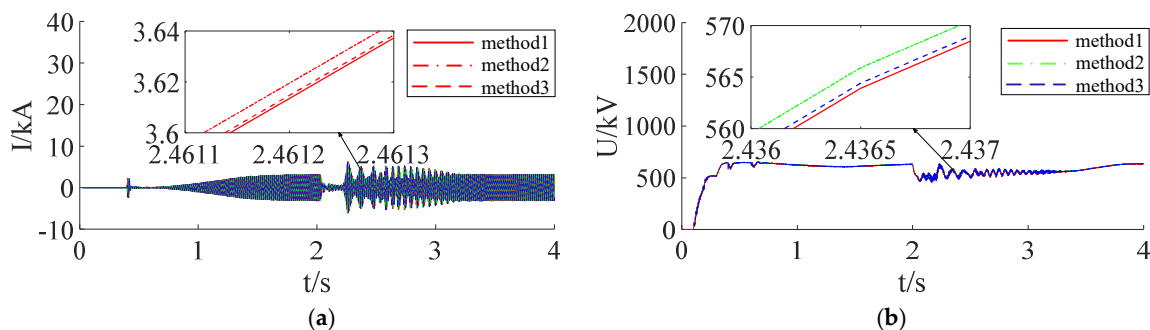
312 **Table 2.** The comparison of single-rate and multi-rate instruction clocks.

313 As can be seen from Table 2, the instruction space occupied by the calculation task of method 1  
 314 has exceeded the allowable space, which cannot meet the requirements of real-time simulation. Both  
 315 of the two multi-rate simulation methods can satisfy the real-time performance of simulation.

316 For proving the accuracy of multi-rate real-time simulation method based on the Norton  
 317 equivalent, it is compared with single-rate off-line simulation and multi-rate real-time simulation  
 318 based on ideal source equivalent.

319 (1) Three phase ground fault in converter bus 3

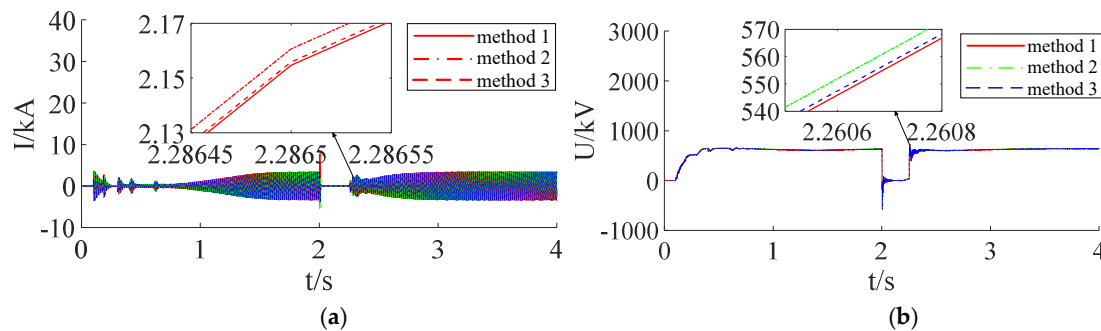
320 When  $t = 2\text{s}$ , three phase metal grounding fault of converter bus 3 is set, and the fault is cleared  
 321 after 0.2s. The simulation result of DC voltage and AC current under single rate and two multi-rate  
 322 methods is shown in Figure 8.



323 **Figure 8.** Three phase ground fault in converter bus 3. (a) AC current. (b) DC voltage  
 324

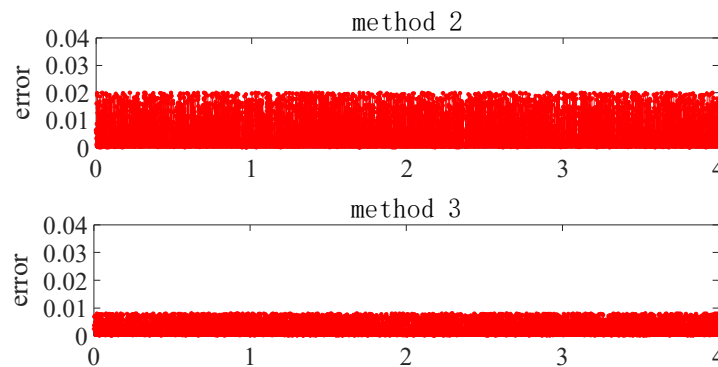
325 (2) The ground fault in DC line

326 When  $t = 2\text{s}$ , the ground fault in DC line is set, and the fault is cleared after 0.2s. The simulation  
 327 result of DC voltage and AC current under single rate and two multi-rate methods is showed in  
 328 Figure 9.  
 329



330  
331  
332 **Figure 9.** The ground fault in DC line. (a) AC current. (b) DC voltage  
333 (3) Error of two multi-rate methods

334 The error between the simulation results of the two multi-rate simulation methods and the  
335 single-rate simulation results is shown in Figure 10. It can be seen that the error of multi-rate  
336 simulation method based on the Norton equivalent is less than 0.8%, and the maximum error of  
337 multi-rate real-time simulation method based on the ideal source equivalence is 2%. The simulation  
338 results of the two multi rate methods meet the simulation correctness, but multi-rate real-time  
339 simulation method based on the Norton equivalence has higher accuracy.



340  
341 **Figure 10.** Error of two multi-rate methods

342 It can be concluded that the accuracy of multi-rate real-time simulation method based on the  
343 Norton equivalence is higher than that based on the ideal source equivalence through the above  
344 pictures. Multi-rate real-time simulation method based on the ideal source equivalence take the  
345 advantage of the characteristic that the inductance current and capacitance voltage in the circuit  
346 cannot be suddenly changed. And the whole system is decoupled by the method of substitution  
347 theorem. The equivalent source of the other system is predicted when the fast and slow system is  
348 calculated, so the accuracy is slightly worse. The conductance of the Norton equivalent circuit is the  
349 true value. It is only necessary to predict the current source of the Norton equivalent circuit of the  
350 slow system during the calculation of the fast system, so the accuracy is higher than multi-rate real-  
351 time simulation method based on the ideal source equivalent.

## 352 4. Conclusions

353 With the widespread application of MMC-based power electronic equipment in power systems,  
354 multi-rate real-time simulation of AC/DC hybrid power system has a broad application prospect in  
355 the field of power system simulation. However, the existing multi-rate simulation methods are not  
356 perfect and have poor accuracy.

357 This paper proposes a multi rate real-time simulation method based on the Norton equivalent,  
358 compared with multi-rate simulation method based on the ideal source equivalent. After the Norton  
359 equivalence of the fast subsystem and the slow subsystem, they are obtained simultaneously at the  
360 junction nodes. In order to reduce the amount of simulation calculation, the Norton equivalent circuit  
361 is obtained by incremental calculation. The data interface between the fast subsystem and the slow  
362 subsystem is realized by extrapolation method. For ensuring the real-time performance of the  
363 simulation, the method that the slow subsystem calculates ahead of the fast subsystem is given for

364 the slow subsystem with a large amount of calculation. Compared with the traditional multi-rate  
 365 simulation methods, the paper proposed method improves the simulation accuracy without losing  
 366 the simulation scale, and has important theoretical and practical significance to research on the real-  
 367 time simulation of the AC/DC hybrid power system.

368 **Author Contributions:** conceptualization, J.Z.; methodology, J.Z.; software, J.Z.; validation, J.Z.; formal analysis,  
 369 J.Z.; investigation, J.Z.; resources, J.Z.; data curation, J.Z.; writing—original draft preparation, J.Z.; writing—review  
 370 and editing, J.Z., B.Z.; visualization, J.Z.; supervision, B.Z.; project administration, B.Z.; funding acquisition, B.Z.

371 **Funding:** This research was funded by the National Natural Science Foundation of China, grant number  
 372 51477114

373 **Conflicts of Interest:** The authors declare no conflict of interest.

## 374 References

- 375 1. Liu, H.B.; Bian, D.; Sun, L.; Yun, Z.J.; Li, Y. Research on Electromechanical-Electromagnetic Transient  
 376 Hybrid Simulation of AC/DC Hybrid System. *Power System Protection and Control*. **2019**, *47*, 39-47.
- 377 2. Li Y.L.; Zhang X., Li, Y.J.; Chen, Z.J.; Wu, M.Q. Current Situation and Challenges of Simulation Technology  
 378 for AC/DC Hybrid Power Grid. *Electric Power Construction*. **2015**, *36*, 1-8.
- 379 3. He, Y.Y.; Zheng, X.D.; Tai, N.L.; Hou, J.X.; Xu, J.; Huang, W.T. Overview of Modeling Methods of LCC-  
 380 HVDC Converter in AC-DC Hybrid Power Grid. *Proceedings of the CSEE*. **2019**, *39*, 3119-3128.
- 381 4. Dong, X.Z.; Tang, Y.; Bu G.Q. Confronting Problem and Challenge of Large Scale AC-DC Hybrid Power  
 382 Grid Operation. *Proceedings of the CSEE*. **2019**, *39*, 3107-3119.
- 383 5. Zhang, M.X. Research on real time multi rate joint simulation technology for power electronic system.  
 384 Master's Degree, Beijing Institute of Technology, Beijing, 2016.
- 385 6. Jost, A.; Niklaus, F.; Min, L. High Fidelity Real-Time Simulation of Multi-Level Converters. 2018  
 386 International Power Electronics Conference, Niigata, Japan, May 20-24, 2018, 2199-2203.
- 387 7. Zhao, J.L.; Liu, J.T.; Li, P. GPU Based Parallel Matrix Exponential Algorithm for Large Scale Power System  
 388 Electromagnetic Transient Simulation. 2016 IEEE Innovative Smart Grid Technologies-Asia, Melbourne,  
 389 Australia November 28- December 1, 110-114.
- 390 8. Lu, F.S.; Song, J.Q.; Yin, F.K.; Zhang, L.L. Overview of CPU/GPU collaborative parallel computing research.  
 391 *Computer Science*. **2011**, *38*, 5-9.
- 392 9. Han, J.; Dong, Y.F.; Miao, S.H.; Liu, Y.L.; Liu, Z.W. MATE-based multi-rate electromagnetic transient  
 393 parallel simulation method for power system sub-network. *High Voltage Engineering*. **2019**, *45*, 1857-1865.
- 394 10. CROW, M.L.; CHEN, J.G. The method for simulation of power system dynamics. *IEEE Trans on Power*  
 395 *Systems*. **1994**, *9*, 1684-1890.
- 396 11. CHEN, J.G.; CROW, M.L. A variable partitioning strategy for the multi-rate method in power system. *IEEE*  
 397 *Trans on Power Systems*. **2008**, *23*, 259-266.
- 398 12. Tang, Y. New Development of Research on Simulation and Modeling of Multi-time Scale Whole Process of  
 399 AC/DC Power System. *Power System Technology*. **2009**, *33*, 1-8.
- 400 13. Moreira, F.A.; Marti, J.R. Latency techniques for time-domain power system transients simulation. *IEEE*  
 401 *Transactions on Power Systems*. **2005**, *20*, 246-253.
- 402 14. Mu, Q; Liang, J.; Zhou, X.X.; Li, G.; Zhang, X. A Node Splitting Interface Algorithm for Multi-rate Parallel  
 403 Simulation of DC Grids. *CSEE Journal of Power and Energy Systems*. **2018**, *4*, 388-397.
- 404 15. Wang, X.; Zhang, B.D.; Chen, M. Multi-rate time Simulation Method Based on RTDS and FPGA Co-  
 405 simulation Platform. *Automation of Electric Power Systems*, **2016**, *40*, 144-150.
- 406 16. Zhai, X.B.; Lin, C.; Gregoire, L.A. Multi-rate Real-time Simulation of Modular Multilevel Converter for  
 407 HVDC Grids Application. IECON 2017 - 43rd Annual Conference of the IEEE Industrial Electronics  
 408 Society,, Beijing, China, October, 29-November, 1, 2017, 1325-1330.
- 409 17. Ou, K.J.; Li, P.F.; Guan, L.; Chai, Z.X.; Zhang, Y.J. Design and Research of Multi-time Scale Hybrid Real-  
 410 Time Simulation System for AC and DC Power Grid. *Southern Power System Technology*. **2017**, *11*, 53-58+64.
- 411 18. Zhang, F.; Huang, W.C.; Li, C.D. MMC generalized fast simulation model suitable for multiple sub-module  
 412 topologies. *Electric Power Automation Equipment*. **2019**, *39*, 129-136+143.
- 413 19. Jost, A.; Niklaus, F. Sub-Cycle Average Models with Integrated Diodes for Real-Time Simulation of Power  
 414 Converters. 2017 IEEE Southern Power Electronics Conference, Puerto Varas, Chile, December 4-7, 2017, 6-  
 415 11.